A bipolaron in a spherical quantum dot with parabolic confinement

1999 J. Phys.: Condens. Matter 11 9033

(http://iopscience.iop.org/0953-8984/11/46/306)

J. Phys.: Condens. Matter **11** (1999) 9033–9043. Printed in the UK PII: S0953-8984(99)06151-2

A bipolaron in a spherical quantum dot with parabolic confinement

E P Pokatilov†, V M Fomin‡§, J T Devreese‡‖, S N Balaban‡ and S N Klimin‡¶

† Laboratory of Multilayer Structure Physics, Department of Theoretical Physics, State University of Moldova, A Mateevici str., 60, MD-2009 Kishinev, Republic of Moldova
‡ Theoretische Fysica van de Vaste Stof, Departement Natuurkunde, Universiteit Antwerpen (UIA), Universiteitsplein 1, B-2610 Antwerpen, Belgium

Received 20 July 1999

Abstract. A theory of bipolaron states in a spherical parabolic potential well is developed applying the Feynman variational principle. The basic parameters of the bipolaron ground state (the binding energy, the number of phonons in the bipolaron cloud, and the bipolaron radius) are studied as functions of the radius R of the potential well. Analytical expressions for bipolaron parameters are obtained at large and small sizes of the quantum well. It is shown that at $R \gg 1$ (where R is expressed in units of the polaron radius), the influence of confinement on the bipolaron binding energy $W(R)$ is described by the function $\sim 1/R^2$, while at small sizes this influence is more complicated: $W(R)$ passes through a maximum in the region $R < 1$.

1. Introduction

The bipolaron problem has been widely discussed for a long time; see e.g. references [1–9]. A detailed outline of this subject is presented in the recent review [10]. The complexity of the polaron problem is enhanced by the fact that the possibility of the existence of the bipolaron is not obvious. The dimensionless Fröhlich constant which characterizes, in particular, the phonon-mediated attraction between two electrons:

$$\alpha = \frac{e^2}{2\hbar\omega_0}\left(\frac{1}{\varepsilon_\infty} - \frac{1}{\varepsilon_0}\right)\left(\frac{2m\omega_0}{\hbar}\right)^{1/2} \tag{1}$$

(where ω_0 is the LO phonon frequency, m is the electron band mass, ε_0 and ε_∞ are static and optical dielectric constants, respectively), and the dimensionless parameter U which characterizes the Coulomb repulsion between them:

$$U = \frac{e^2(m\omega_0/\hbar)^{1/2}}{\varepsilon_\infty\hbar\omega_0} \tag{2}$$

§ Permanent address: Laboratory of Multilayer Structure Physics, Department of Theoretical Physics, State University of Moldova, A Mateevici str., 60, MD-2009 Kishinev, Republic of Moldova. Also at: Technische Universiteit Eindhoven, PO Box 513, 5600 MB Eindhoven, The Netherlands.
‖ Also at: Universiteit Antwerpen (RUCA), Groenenborgerlaan 171, B-2020 Antwerpen, Belgium, and Technische Universiteit Eindhoven, PO Box 513, 5600 MB Eindhoven, The Netherlands.
¶ Present address: Theoretische Fysica van de Vaste Stof, Departement Natuurkunde, Universiteit Antwerpen (UIA), Universiteitsplein 1, B-2610 Antwerpen, Belgium.

0953-8984/99/469033+11$30.00

are related to each other by the equation [10]

$$U = \frac{\sqrt{2}\alpha}{1-\eta} \tag{3}$$

where $\eta = \varepsilon_\infty/\varepsilon_0$. Due to the fact that $\varepsilon_0 > \varepsilon_\infty$, the inequality $U \geqslant \sqrt{2}\alpha$ is obvious. From this inequality, generally speaking, the domination of repulsion follows. Indeed, when the distance between two electrons $|\boldsymbol{r}_2 - \boldsymbol{r}_1|$ is large in comparison with the polaron radius $R_\mathrm{p} = (\hbar/m\omega_0)^{1/2}$, such that each electron moves in a separate potential well, the Coulomb repulsion obviously exceeds the phonon-mediated attraction. In the opposite case $|\boldsymbol{r}_2 - \boldsymbol{r}_1| \ll R_\mathrm{p}$, the repulsion also exceeds the attraction, since the Coulomb potential diverges when $|\boldsymbol{r}_2 - \boldsymbol{r}_1| \to 0$. Only at intermediate distances, $|\boldsymbol{r}_2 - \boldsymbol{r}_1| \sim R_\mathrm{p}$, at large α, may the attraction exceed the repulsion. Therefore, when two electrons are confined together in a potential well, one can expect the conditions of the bipolaron stability to be improved at relevant sizes R of the well, because confinement turns off the region $|\boldsymbol{r}_2 - \boldsymbol{r}_1| > R$, where repulsion between two electrons dominates.

Two new circumstances have stimulated the bipolaron theory: the progress in the technology of fabrication of mesoscopic nanostructures such as quasi-2D (quantum wells and superlattices), quasi-1D (quantum wires), and quasi-0D (quantum dots) structures, and the advancing of the hypothesis that bipolaron excitations might play a role in processes occurring in the high-temperature superconductors. The present research has been motivated also by the recent advances in the creation of nanocrystals with a strong ionic coupling [11].

The basic bipolaron parameters are the following. The bipolaron stability region is determined by the inequality $W > 0$ for the bipolaron binding energy:

$$W \equiv 2E_\mathrm{p} - E_\mathrm{bip}. \tag{4}$$

Here E_p and E_bip are the free-polaron and bipolaron ground-state energies, respectively. The functions $\alpha_c(\eta, R)$ and $\eta_c(\alpha, R)$, describing the boundaries of the bipolaron stability region, are found from the equation

$$W(\alpha, \eta, R) = 0. \tag{5}$$

When $R \sim R_\mathrm{p}$, with the result that two electrons are confined near each other independently of the sign of W, we can attach a specific meaning to the inequality $W > 0$ by considering an array of N_0 quantum dots which are separated by high energy barriers and contain N electrons ($N < N_0$). In thermodynamical equilibrium, the ratio of the number of quantum dots with one electron (polarons) to the number of those with two electrons (bipolarons) is equal to $\exp(-W/k_BT)$, so at $W > 0$, the number of bipolarons is larger than the number of polarons.

According to different theoretical treatments [4–10] and for intuitive reasons, the bipolaron binding energy is an increasing function of α and a decreasing function of η. It will be shown that the function $\eta_c(\alpha, R)$ starts from $\eta_c = 0$ at $\alpha = \alpha_\mathrm{min}(R) \neq 0$, grows with increasing α, and tends to the upper limit η_max at $\alpha \to \infty$. The bipolaron stability region is then determined by the inequalities $\alpha \geqslant \alpha_\mathrm{min}(R)$ and $0 \leqslant \eta < \eta_c(\alpha, R)$.

Let us adduce typical values of the parameters $\alpha_\mathrm{min,3D}$ and $\eta_\mathrm{max,3D}$ of the bulk (3D) bipolaron: $\alpha_\mathrm{min,3D} = 6.8$ and $\eta_\mathrm{max,3D} = 0.14$ were found by Verbist, Peeters, and Devreese [12, 13] and by Verbist, Smondyrev, Peeters, and Devreese [14]. Adamowski [7] obtained $\alpha_\mathrm{min,3D} = 7.3$ and $\eta_\mathrm{max,3D} = 0.14$.

The bipolaron theory developed for pure 2D [15, 16] and 1D [16] models shows that the bipolaron stability region broadens when the dimensionality is reduced. For these systems, the following parameters were obtained: $\alpha_\mathrm{min,2D} = 2.9$, $\eta_\mathrm{max,2D} = 0.158$ (reference [15]); $\alpha_\mathrm{min,1D} = 0.9$, $\eta_\mathrm{max,1D} = 0.764$ (reference [17]).

Bipolaron states were investigated in a quantum well [18, 19] and in a quantum wire [20] as functions of the characteristic size of the system: the width and the radius, respectively. Although the polaron theory for the quantum dot is developed in detail in references [21–24], publications on bipolarons in quantum dots, to the best of our knowledge, are lacking, except the recent reference [25], the results of which are analysed in section 5.

The goal of the present investigation is to determine the region of bipolaron stability and to study basic parameters characterizing the bipolaron ground state as a function of the confinement for quantum dots, where a transition from 3D to 0D is realized. The Feynman variational method is used in order to study the problem for arbitrary values of α.

The paper is organized as follows. In section 2, general formulae for parameters of a bipolaron in the spherical confinement potential are deduced. In section 3, the basic parameters of the bipolaron ground state are obtained. Limiting cases of strong and weak confinement are studied in detail. The numerical and analytical results obtained are discussed in section 4.

2. General theory

We analyse the bipolaron problem taking into account both the electron–phonon interaction and the Coulomb repulsion between two electrons confined in a quantum dot. The Lagrange function of the system is

$$L = \sum_{i=1}^{3}\sum_{n=1,2}\frac{m\dot{x}_{i,n}^2}{2} - \sum_{n=1,2}\mathcal{U}(\boldsymbol{r}_n) - \frac{e^2}{\varepsilon_\infty|\boldsymbol{r}_1-\boldsymbol{r}_2|} + \frac{1}{2}\sum_{\boldsymbol{k}}(\dot{w}_{\boldsymbol{k}}^2-\omega_0^2 w_{\boldsymbol{k}}^2) - \sum_{n=1,2}\sum_{\boldsymbol{k}}\gamma_{\boldsymbol{k}}(\boldsymbol{r}_n)w_{\boldsymbol{k}} \tag{6}$$

where $\boldsymbol{r}_n(x_{1n},\ldots,x_{3n})$ is the radius vector of the nth electron ($n=1,2$), $\mathcal{U}(\boldsymbol{r})$ is the potential energy of an electron in the potential well, $w_{\boldsymbol{k}}$ are the normal coordinates of longitudinal optical (LO) phonon modes. The amplitudes of the electron–phonon interaction are taken in the Fröhlich form:

$$\gamma_{\boldsymbol{k}}(\boldsymbol{r}) = 2\sqrt{\frac{2\pi\hbar\omega_0\alpha}{V}}\frac{\omega_0}{k}\left(\frac{\hbar}{2m\omega_0}\right)^{1/4}\exp(\mathrm{i}\boldsymbol{k}\cdot\boldsymbol{r}) \tag{7}$$

where V is the volume of the system. In this paper, the so-called 3D phonon approximation is used, according to which the interaction of an electron with both bulk-like and interface phonons is replaced by that with 3D phonons. This often-used approach is adequate because any integral polaron or bipolaron effect, resulting from a summation over all phonon modes, appears to be only weakly dependent on the details of the phonon spectra. It should also be mentioned that the system under consideration simulates realistic structures with relatively smooth interface barriers, where interface-like phonon modes can appear, which are smoothly distributed in space rather than localized near a sharp boundary as is the case for interface modes.

For studying the bipolaron problem at arbitrary values of α, the Feynman variational approach [26] is the most appropriate method. The trial Lagrange function is written as

$$L_{tr} = \frac{1}{2}\sum_{i=1}^{3}\sum_{n=1,2}\left[m\dot{x}_{i,n}^2 + M\dot{X}_{i,n}^2 - k(x_{i,n}-X_{i,n})^2 - k'(x_{i,n}-X_{i,\bar{n}})^2\right] + \sum_{i=1}^{3}K(x_{i1}-x_{i2})^2 - \sum_{n=1,2}\mathcal{W}(\boldsymbol{r}_n) \tag{8}$$

where the X_{in} are coordinates of the nth fictitious particle. This model imitates the interaction of electrons with phonons and with each other by using elastic bonds as shown in figure 1. The mass M and the force constants k, k', K play the roles of variational parameters. For $n = 1$, $\bar{n}$ takes the value 2, and for $n = 2$, $\bar{n}$ is equal to 1. The potential well $\mathcal{U}(\boldsymbol{r})$ in equation (6) is simulated by a parabolic function:

$$\mathcal{W}(\boldsymbol{r}) = \frac{m\Omega^2}{2}\sum_{i=1}^{q} x_i^2. \tag{9}$$

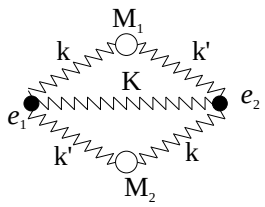

Figure 1. A schematic diagram of the trial system which contains two electrons connected with two fictitious particles through the elastic attraction and models the Coulomb interaction as the elastic repulsion.

The basis of the Feynman variational method is the Jensen–Feynman inequality [26]:

$$\langle \exp(S - S_{tr})\rangle_{S_{tr}} \geqslant \exp\langle S - S_{tr}\rangle_{S_{tr}} \tag{10}$$

where the angular brackets denote averaging over electron paths:

$$\langle G\rangle_{S_{tr}} = \left(\mathrm{Tr}\int \mathrm{D}\boldsymbol{r}\; G[\boldsymbol{r}]\exp(S_{tr})\right)\Big/\left(\mathrm{Tr}\int \mathrm{D}\boldsymbol{r}\;\exp(S_{tr})\right). \tag{11}$$

Here S and S_{tr} are the electron action functionals obtained after integration over phonon variables and over coordinates of fictitious particles, respectively. At low temperatures, the variational bipolaron energy is calculated using the expression

$$E_{\mathrm{bip}} = E_{tr} - \lim_{\beta\to\infty}\frac{\langle S - S_{tr}\rangle_{S_{tr}}}{\beta} \tag{12}$$

where E_{tr} is the ground-state energy of the trial system with the Lagrangian (8); $\beta = 1/k_B T$ is the inverse temperature.

The trial Lagrange function (8) consists of three independent parts:

$$L_{tr} = \sum_{i=1}^{3} L_i.$$

Each part L_i is a function of four variables x_{i1}, x_{i2}, X_{i1}, X_{i2}. Let us introduce unified notation for the coordinates of electrons and of fictitious particles: $\tilde{x}_{i1} = x_{i1}$, $\tilde{x}_{i2} = x_{i2}$, $\tilde{x}_{i3} = X_{i1}$, $\tilde{x}_{i4} = X_{i2}$. It follows from the form of the trial Lagrangian (8) with equation (9) that the groups of variables $\tilde{x}_{ij}$ with different indices i are dynamically independent of each other. They are related to the normal variables ξ_{ij} by the unitary transformation

$$\tilde{x}_{ij} = \sum_{j'=1}^{4} d_{jj'}\xi_{ij'} \qquad i = 1, 2, 3 \tag{13}$$

with 4×4 matrices $\|d_{jj'}\|$ ($j, j' = 1, \ldots, 4$). From the equations of motion for the group of coordinates $\tilde{x}_{ij}$ ($j = 1, \ldots, 4$) with a fixed i, the eigenfrequencies are obtained:

$$\omega_j^2 = \begin{cases} \dfrac{1}{2}\left\{\left(1+\dfrac{M}{m}\right)v^2 + \Omega^2 - (-1)^j\sqrt{\left[\left(1-\dfrac{M}{m}\right)v^2 - \Omega^2\right]^2 + 4\dfrac{M}{m}v^4}\right\} & j = 1, 2 \\ \dfrac{1}{2}\left\{\left(1+\dfrac{M_i}{m}\right)v^2 + \Omega^2 - 2\dfrac{K}{m}\right. & \\ \qquad \left. - (-1)^j\sqrt{\left[\left(1-\dfrac{M_i}{m}\right)v^2 - \Omega^2 + 2\dfrac{K}{m}\right]^2 + 4\dfrac{(k-k')^2}{mM}}\right\} & j = 3, 4 \end{cases} \tag{14}$$

where $v^2 = (k+k')/M$. The matrix elements of the unitary transformation (13) are as follows:

$$\begin{aligned} d_{11}^2 &= \frac{\omega_1^2 - v^2}{2(\omega_1^2 - \omega_2^2)} & d_{12}^2 &= \frac{v^2 - \omega_2^2}{2(\omega_1^2 - \omega_2^2)} \\ d_{13}^2 &= \frac{\omega_3^2 - v^2}{2(\omega_3^2 - \omega_4^2)} & d_{14}^2 &= \frac{v^2 - \omega_4^2}{2(\omega_3^2 - \omega_4^2)} \\ d_{2j'} &= s_{j'}d_{1j'} & d_{3j'} &= \frac{k + s_{j'}k'}{M(v^2 - \omega_{j'}^2)}d_{1j'} \\ d_{4j'} &= s_{j'}d_{3j'} & & \\ s_j &= \begin{cases} 1 & j = 1, 2 \\ -1 & j = 3, 4. \end{cases} & & \end{aligned} \tag{15}$$

Note that the Coulomb interaction gives a contribution to frequencies with $j = 3, 4$. It is easy to see from equation (14) that under the conditions of strong confinement, the eigenfrequencies ω_j are determined mainly by the parameter Ω.

The action functionals S and S_{tr} in equations (10)—(12) contain the potential energies $\mathcal{U}$ and $\mathcal{W}$, respectively. The shape of a real potential $\mathcal{U}$ may differ from that of the model quadratic potential (9), but the averaged difference $\langle \mathcal{U} - \mathcal{W} \rangle_{S_{tr}}$ can be omitted as long as it is small when compared with the rest of $\langle S - S_{tr} \rangle_{S_{tr}} / \beta$.

The averaging procedure in equation (12) is carried out by path integration and leads to the following form of the variational bipolaron energy:

$$E_{\text{bip}} = 3B + C + P. \tag{16}$$

Here the term $3B$ includes averaged kinetic energies of two electrons and of two 'fictitious' particles as well as the averaged potential energy of the elastic interaction of these four particles:

$$B = \frac{1}{2}\sum_{j=1}^{4}\omega_j\left(1 - \frac{\omega_j^2 - \Omega^2}{\omega_j^2}d_{1j}^2\right) - v. \tag{17}$$

In equations (16), (17) and further on, Feynman units are used: $\hbar\omega_0$ for energies; ω_0 for frequencies; $R_{\text{p}} = (\hbar/m\omega_0)^{1/2}$ for lengths.

The averaged potential energy of the Coulomb electron repulsion is

$$C = \frac{\alpha}{(1-\eta)\pi^2}\mathcal{K}_2(0) \tag{18}$$

and the averaged energy of the electron–phonon interaction is

$$P = -\frac{\alpha}{\pi^2}\sum_{n=1,2}\int_0^\infty \mathrm{d}\tau\ \mathrm{e}^{-\tau}\mathcal{K}_n(\tau) \tag{19}$$

where

$$\mathcal{K}_n(\tau) = \int_{-\infty}^{\infty} \frac{1}{k^2} \exp\left[-k^2 A_n(\tau)\right] \prod_{i=1}^{3} \mathrm{d}k_i. \tag{20}$$

The functions $A_n(\tau)$ are determined as follows:

$$r A_n(\tau) = \left\{ \sum_{j=1,2} \frac{d_{1j}^2}{\omega_j} \left[1 - \exp(-\omega_j \tau)\right] + \sum_{j=3,4} \frac{d_{1j}^2}{\omega_j} \left[1 + (-1)^n \exp(-\omega_j \tau)\right] \right\} \qquad n = 1, 2. \tag{21}$$

In order to find the bipolaron energy, it is necessary to minimize the function E_{bip} given by equation (16) over four independent variational parameters ω_j, $j = 1, \ldots, 4$, which are used instead of the mass M and the force constants k, k', K.

The number of phonons in the bipolaron cloud is determined by the general expression from reference [27]:

$$N_{\mathrm{ph}} = \left\langle \frac{\partial S}{\partial(\hbar\omega_0)} \right\rangle_{S_{tr}} \tag{22}$$

which gives, in the case under consideration,

$$N_{\mathrm{ph}} = \frac{\alpha}{\pi^2} \sum_{n=1,2} \int_0^{\infty} \mathcal{K}_n(\tau) \mathrm{e}^{-\tau} \tau \, \mathrm{d}\tau. \tag{23}$$

Calculations by means of equation (23) are performed using the results of minimization of the bipolaron energy.

3. Bipolaron parameters

The following form for the variational bipolaron energy results from the general expression (16):

$$E_{\mathrm{bip}} = \frac{3}{2} \sum_{j=1}^{4} \omega_j \left(1 - \frac{\omega_j^2 - \Omega^2}{\omega_j^2} a_j\right) - 3v + \frac{2\alpha}{(1-\eta)\left[\pi A_2(0)\right]^{1/2}} - \frac{2\alpha}{\sqrt{\pi}} \int_0^{\infty} \mathrm{e}^{-\tau} \sum_{n=1,2} \left[A_n(\tau)\right]^{-1/2} \mathrm{d}\tau \tag{24}$$

where the function $A_n(\tau)$, according to equation (21), is

$$A_n(\tau) = \sum_{j=1}^{2} a_j \frac{1 - \exp(-\omega_j \tau)}{\omega_j} + \sum_{j=3}^{4} a_j \frac{1 + (-1)^n \exp(-\omega_j \tau)}{\omega_j} \qquad n = 1, 2$$

with coefficients

$$a_1 = \frac{1}{2} \frac{\omega_1^2 - v^2}{\omega_1^2 - \omega_2^2} \qquad a_2 = \frac{1}{2} \frac{v^2 - \omega_2^2}{\omega_1^2 - \omega_2^2} \qquad a_3 = \frac{1}{2} \frac{\omega_3^2 - v^2}{\omega_3^2 - \omega_4^2} \qquad a_4 = \frac{1}{2} \frac{v^2 - \omega_4^2}{\omega_3^2 - \omega_4^2}. \tag{25}$$

A schematic representation of the different normal oscillations of the trial system is shown in figure 2. As Ω tends to zero, the normal oscillation with the frequency ω_2 transforms to a translational motion with $\omega_2 = 0$ of the bipolaron as a whole. Frequencies ω_1, ω_3, and ω_4 correspond to the internal degrees of freedom of the bipolaron. In particular, as follows from equation (14), a normal oscillation with the frequency ω_1 describes such a relative motion of electrons and of fictitious particles in the case where both the distance between electrons and that between fictitious particles do not change.

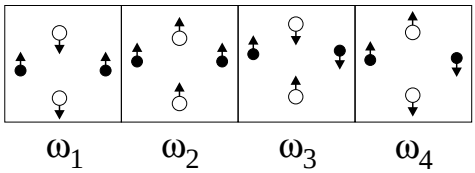

Figure 2. A schematic representation of the normal oscillations of the trial system in a quantum dot.

The phonon number in the bipolaron cloud is calculated using the expression

$$N_{\rm ph} = \frac{2\alpha}{\sqrt{\pi}} \int_0^\infty \tau {\rm e}^{-\tau} \sum_{n=1,2} [A_n(\tau)]^{-1/2} \, {\rm d}\tau \tag{26}$$

which follows from equation (23). The radius of the bipolaron is defined as

$$R_{\rm bip} = \sqrt{\frac{1}{3} \left\langle (\boldsymbol{r}_1 - \boldsymbol{r}_2)^2 \right\rangle_{S_{tr}}} \tag{27}$$

and turns out to be

$$R_{\rm bip} = \sqrt{\frac{\omega_3\omega_4 + v^2}{2\omega_3\omega_4(\omega_3 + \omega_4)}}. \tag{28}$$

In the limiting case of a weak confinement, the expression in (24) tends to that known from references [12, 13] for the variational energy of a 3D bipolaron. For a large radius of the quantum dot and for a strong polaron coupling ($\alpha \gg 1$), the bipolaron binding energy is reduced to the form

$$W = W_{\rm 3D} + \frac{3}{2\alpha^2 R^2} \left(\frac{9\pi}{2} - \frac{1}{\widetilde{\omega}_3} \right) \tag{29}$$

where $W_{\rm 3D}$ is the bipolaron binding energy in the bulk. The parameter $\widetilde{\omega}_3$ is determined (see [28]) by

$$\widetilde{\omega}_3 = \frac{128}{9\pi} \left[1 - \zeta^2(U) \right]^3 \qquad \zeta(U) = \frac{U}{16\alpha} + \frac{1}{2} \sqrt{2 + \left(\frac{U}{8\alpha} \right)^2}. \tag{30}$$

It can be shown that $\tilde{\omega}_3 > 2/9\pi$. Hence, a weak confinement leads to an increase of the bipolaron binding energy when compared with $W_{\rm 3D}$.

It is worth mentioning that in the opposite limit of a strong confinement, the bipolaron binding energy of the 'squeezed' state ($R \ll 1$) is found to be negative:

$$W(R) = -\frac{2\alpha\eta}{\sqrt{\pi}(1-\eta)R}. \tag{31}$$

Hence, this state is outside the region of bipolaron stability. As long as under strong 3D confinement the average distance between two electrons is small, the Coulomb repulsion exceeds the phonon-mediated attraction. Consequently, in this case $W(R)$ is negative. With decreasing R, the bipolaron binding energy initially rises (cf. equation (29)) and then falls (cf. equation (31)); therefore it has a maximum $W_{\rm max}$.

4. Discussion of numerical results

The region with the Fröhlich coupling constant ranging from 2 to 4 is chosen for the numerical work in order to include the values of α corresponding to some specific substances with small η (for example, TiO_2: $\alpha = 2.03$, $\eta = 0.035$ [29]; TlCl: $\alpha = 2.56$, $\eta = 0.133$ [30]; BaO: $\alpha = 3.23$, $\eta = 0.118$ [29]; LiBr: $\alpha = 4.15$, $\eta = 0.24$ [30]). In order to compare the properties of a bipolaron in quasi-linear structures in three and two dimensions with each other, cylindrical and planar quantum wires are analysed (see figure 2).

In figures 3(a) and 3(b), graphs of the bipolaron binding energies in quantum dots are represented for given values of α and η. Numerical calculations show that, with strengthening confinement, the bipolaron binding energy $W(R) \to 0$ for $\eta = 0$, whereas for $\eta \neq 0$, this function tends to a negative value determined by equation (31) at $R \ll 1$. Both figure 3(a) and figure 3(b) demonstrate that a stable bipolaron in a quantum dot appears at a smaller value of α than $\alpha_{\mathrm{min,3D}} = 6.8$ and $\alpha_{\mathrm{min,2D}} = 2.9$. In the region $R < 1$, with decreasing radius, the function $W(R)$ passes through a maximum. In accordance with this behaviour of $W(R)$, the critical value $\alpha_c(\eta, R)$ as a function of R passes through a minimum in the region $R < 1$ and grows further with decreasing R at a fixed $\eta \neq 0$; see figure 4. For $0 \leqslant \eta \leqslant 0.02$ this minimum is lower than $\alpha_{\mathrm{min,2D}}$, so the inequality $\alpha_c(\eta, R) < \alpha_{\mathrm{min,2D}}$ is obeyed for the R-values ranging from 0.7 at $\eta = 0.02$ up to 2 at $\eta = 0$. Note that the positions of the minima α_{min} on those

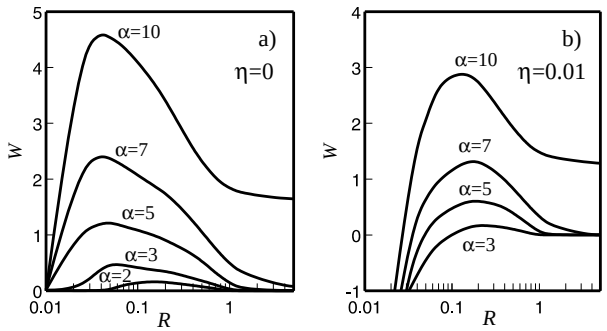

Figure 3. Plots of the binding energy of a bipolaron versus the radius of a quantum dot at different values of the coupling constant α for $\eta = 0$ (panel (a)) and $\eta = 0.01$ (panel (b)).

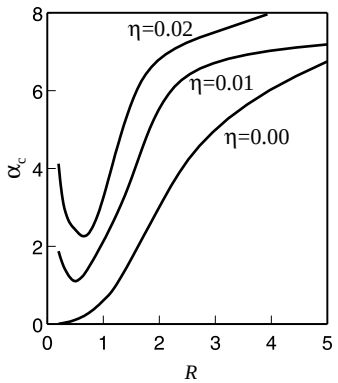

Figure 4. Plots of the critical value of the coupling constant α_c versus the radius of a quantum dot at different values of the parameter η.

graphs are shifted to larger R-values relatively to the positions of the respective maxima $W_{\max}$ as given by figures 3(a), 3(b).

At $\eta = 0, \alpha_{\min}(R)$ increases monotonically with the radius. It follows from the comparison of the $\alpha_{\min}(R)$ values, calculated for a quantum dot, with those obtained for a cylindrical quantum wire (see figure 2 of [20]) that $\alpha_{\min,\mathrm{QD}}(R) < \alpha_{\min,\mathrm{QW}}(R)$ at equal radii of the quantum dot and of the quantum wire. So, the conditions of bipolaron stability are *more favourable in a quantum dot* than in a cylindrical quantum wire.

Our treatment, both analytical and numerical, implies the existence of $W_{\max}$ and of $\alpha_{\min}$ for a quantum dot. This result is in contrast with that obtained in reference [25]. Bipolaron parameters are calculated in reference [25] by the strong-coupling variational method; as a consequence, $W(R)$ is shown to diminish monotonically with decreasing R. As long as $W(R) \to W_{3\mathrm{D}}$ for $R \to \infty$, then $W(R)$ of reference [25] is always less than $W_{3\mathrm{D}}$. This assertion looks questionable when compared to the conclusion of the present work, that confinement can enhance the bipolaron binding energy; when the radius of a quantum dot is of the same order of magnitude as the polaron radius. It is found in the present paper and in references [17–19] that confinement to two dimensions as well as to one dimension enhances the bipolaron binding energy; moreover, $W_{1\mathrm{D}} > W_{2\mathrm{D}} > W_{3\mathrm{D}}$. Thus, in all known cases, both the diminution of the confinement domain and the reduction of the dimensionality of the structure lead to an increase of the bipolaron binding energy.

The dependence of N_{ph} on the radius of a quantum dot is shown in figure 5. It is obvious that the function $N_{\mathrm{ph}}(R, \alpha)$ monotonically increases with decreasing R owing to the growth of the electron charge density. This behaviour arises because of the conditions of strong size quantization, when the Coulomb repulsion practically does not influence the distribution of the electron charge density.

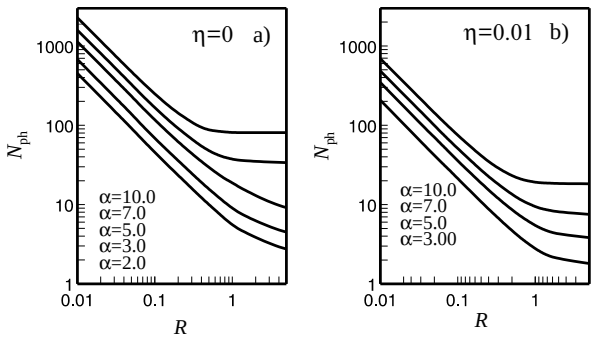

Figure 5. The number of phonons in the bipolaron cloud as a function of the radius of a quantum dot at different values of the coupling constant for $\eta = 0$ (panel (a)) and $\eta = 0.01$ (panel (b)).

The graphs of R_{bip} as a function of R for a quantum dot are represented in figure 6(a) ($\eta = 0$) and figure 6(b) ($\eta = 0.01$). For large R, two different types of two-electron state can be distinguished according to the value of α. For $\alpha \leqslant 5$, the correlation between electrons is small, and the system consists of two weakly interacting polarons. On reducing the quantum dot size, bends appear on the curves with $\alpha = 2, 3, 5$. Those bends are more pronounced on the graph with $\alpha = 5, \eta = 0$. This feature confirms the fact that the confinement strengthening stimulates the phonon-mediated attraction between electrons. In the same domain of R, as seen from the graphs in figures 3(a), 3(b), the binding energy W starts to increase rapidly with decreasing R. For $\alpha \geqslant 7$, there is a strong correlation of the motion of electrons in the bipolaron, even in the absence of confinement. In this case, a decrease in R does not

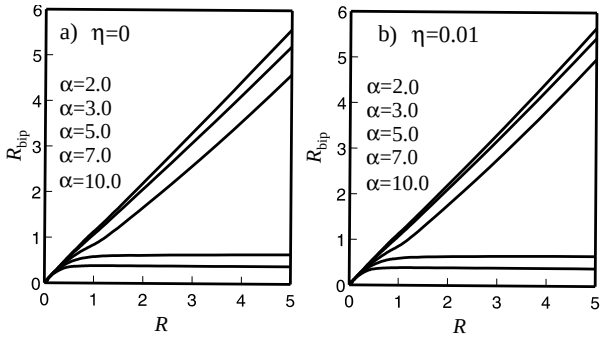

Figure 6. The bipolaron radius as a function of the quantum dot radius R at different values of the coupling constant for $\eta = 0$ (panel (a)) and $\eta = 0.01$ (panel (b)).

influence $R_{\rm bip}$ until $R \simeq R_{\rm bip,3D}$. For small values of R and for an arbitrary α, $R_{\rm bip}$ reduces proportionally to R.

To summarize the results, the reduction of the quantum dot size strengthens not only the efficiency of the electron–phonon interaction for each electron separately but also the phonon-mediated attraction between electrons. As a consequence, the phonon numbers $N_{\rm ph}$ in bipolaron clouds monotonically rise. The radius $R_{\rm bip}$ in a quantum dot experiences a direct influence of the confinement. For $R < R_{\rm bip,3D}$, the bipolaron radius vanishes proportionally to R. For $R > R_{\rm bip,3D}$, in the domain where $\alpha \approx \alpha_{\rm min,3D}$, there is a sharp transformation of the function $R_{\rm bip}(R)$. This transformation describes a *transition* from a 3D bipolaron to two independent polarons whose radii are determined by the confinement. It is natural that for large R, the bipolaron characteristics reflect the well known difference between the regimes of strong and weak electron–phonon coupling, but for small R and $\alpha R < 1$ this difference disappears. Such a quantum state of two electrons can be referred to as a 'squeezed' bipolaron.

Technological possibilities for fabricating quantum dots of small radius are demonstrated in references [31, 32], where CdSe nanocrystals of spherical shape with $R \sim 1$ nm are investigated.

5. Conclusions

The analytical and numerical analysis performed of the influence of confinement on the bipolaron binding energy has shown that stable bipolaron states are possible even for intermediate values of α ($\alpha \sim 2$) and for not-too-small values of η ($\eta \sim 0.1$) in nanostructures whose sizes are of the same order as the polaron radius $R_{\rm p}$.

Acknowledgments

We thank V N Gladilin for valuable discussions. This work was supported by the Interuniversitaire Attractiepolen—Belgische Staat, Diensten van de Eerste Minister—Wetenschappelijke, technische en culturele Aangelegenheden; Bijzonder Onderzoeksfonds (BOF) NOI 1997 of the Universiteit Antwerpen; PHANTOMS Research Network; FWO-V project No G.0287.95 and the WOG WO.025.99N (Belgium). SNK acknowledges financial support from the UIA. EPP, SNK, and SNB acknowledge with gratitude the kind hospitality enjoyed during their visits to the UIA in the framework of the common research project supported by PHANTOMS.

References

[1] Landau L D 1933 *Phys. Z. Sowjetunion* **3** 664 (Engl. Transl. 1965 *Collected Papers* (New York: Gordon and Breach) pp 67–8)
[2] Pekar S I 1963 *Research on Electron Theory in Crystals* (Washington, DC: US AEC)
[3] Vinetskii V L and Giterman M S 1957 *Zh. Eksp. Teor. Fiz.* **33** 730
[4] Mukhomorov V K 1982 *Fiz. Tekh. Poluprov.* **16** 1095 (Engl. Transl. 1982 *Sov. Phys.—Semicond.* **16** 799)
[5] Suprun S G and Moizhes B Ya 1982 *Fiz. Tverd. Tela* **24** 1571 (Engl. Transl. 1982 *Sov. Phys.–Solid State* **24** 903)
[6] Vinetskii V L, Meredov O and Yanchuk V A 1989 *Teor. Eksp. Khim.* **25** 641
[7] Adamowski J 1988 *Acta Phys. Pol.* A **73** 345
Adamowski J 1985 *Phys. Rev.* B **39** 3649
[8] Sil S, Giri A K and Chatterjee A 1991 *Phys. Rev.* B **43** 12 642
[9] Kashirina N I, Mozdor E V, Pashitskii E A and Sheka V I 1995 *Izv. Akad. Nauk Ser. Fiz.* **59** 127
[10] Devreese J T 1996 Polarons *Encyclopedia of Applied Physics* vol 14 (New York: VCH) pp 383–413
[11] Hudgins R R, Durourd P, Tenenbaum J M and Jarrold M F 1997 *Phys. Rev. Lett.* **78** 4213
[12] Verbist G, Peeters F M and Devreese J T 1990 *Solid State Commun.* **76** 1005
[13] Verbist G, Peeters F M and Devreese J T 1991 *Phys. Rev.* B **43** 2712
[14] Verbist G, Smondyrev M A, Peeters F M and Devreese J T 1992 *Phys. Rev.* B **45** 5262
[15] Vansant P, Smondyrev M A, Peeters F M and Devreese J T 1994 *J. Phys. A: Math. Gen.* **27** 7925
[16] Luczak F, Brosens F and Devreese J T 1995 *Phys. Rev.* B **52** 12 743
[17] Vansant P, Peeters F M, Smondyrev M A and Devreese J T 1994 *Phys. Rev.* B **50** 12 524
[18] Pokatilov E P, Beril S I, Fomin V M and Ryabukhin G Iu 1992 *Phys. Status Solidi* b **169** 429
[19] Pokatilov E P, Beril S I, Fomin V M, Ryabukhin G Iu and Goryachkovskii G R 1992 *Phys. Status Solidi* b **171** 437
[20] Pokatilov E P, Fomin V M, Balaban S N, Klimin S N, Fai L C and Devreese J T 1998 *Superlatt. Microstruct.* **23** 331
[21] Klimin S N, Pokatilov E P and Fomin V M 1994 *Phys. Status Solidi* b **184** 373
[22] Wendler L, Chaplik A V, Haupt R and Hipolito O 1993 *J. Phys.: Condens. Matter* **5** 4817
[23] Sahoo S 1996 *Z. Phys.* B **101** 97
[24] Pokatilov E P, Fomin V M, Devreese J T, Balaban S N and Klimin S N 1999 *Physica* E **4** 156
[25] Mukhopadhyay S and Chatterjee A 1996 *J. Phys.: Condens. Matter* **8** 4017
[26] Feynman R P and Hibbs A R 1965 *Quantum Mechanics and Path Integrals* (New York: McGraw-Hill)
[27] Peeters F M and Devreese J T 1985 *Phys. Rev.* B **31** 4890
[28] Smondyrev M A, Devreese J T and Peeters F M 1995 *Phys. Rev.* B **51** 15 008
[29] Firsov Yu A (ed) 1975 *Polarony* (Moscow: Nauka) p 424
[30] Kartheuser E 1972 *Polarons in Ionic Crystals and Polar Semiconductors* ed J T Devreese (Amsterdam: North-Holland) pp 717–33
[31] Nirmal M, Murray C B, Norris D J and Bawendi M G 1993 *Z. Phys.* D **26** 361
[32] Norris D J, Efros Al L, Rolen M and Bawendi M G 1996 *Phys. Rev.* B **53** 16 347